Inorg. Chem. **2007**, *46*, 3946–3955

Hexaazamacrocyclic Nickel and Copper Complexes and their Reactivity with Tetracyanoquinodimethane

Loreto Ballester,[†] Angel Gutiérrez,*[,†] M. Felisa Perpiñán,[†] Ana E. Sánchez,[†] Marina Fonari,[‡] and Maria Gdaniec[§]

Departamento de Química Inorgánica I, Facultad de Ciencias Químicas, Universidad Complutense, 28040-Madrid, Spain, Institute of Applied Physics, Academy of Science of Moldova, Academy Str. 5, Chisinau, MD 2028, Moldova, and Department of Chemistry, Adam Mickiewicz University, Poznań, Poland

Received October 20, 2006

The hexaazamacrocycle 1,4,7,10,13,16-hexaazacyclooctadecane, [18]ane-N_6, forms mono- and dinuclear derivatives with copper chloride depending on the reaction stoichiometries and times. The mononuclear derivative, [Cu([18]-ane-N_6)]$Cl_2\cdot H_2O$, presents the macrocycle wrapped around the metal atom in a distorted octahedral coordinative environment, while the dinuclear derivative, [Cu_2([18]ane-N_6)Cl_2]$Cl_2\cdot 4H_2O$, is formed by a central Cu_2Cl_2 core surrounded by an almost planar macrocycle. The crystal structure of both derivatives is stabilized by a network of hydrogen bonds involving the amine macrocyclic groups, the chloride anions, and the crystallization water molecules. The copper atoms in the dinuclear derivative show a strong antiferromagnetic coupling, as expected for the crystal structure parameters. A mononuclear nickel derivative has also been obtained from nickel nitrate by following the same synthetic procedure. These compounds react with TCNQ salts with formation of two types of derivatives, [M([18]ane-N_6)]$(TCNQ)_2$ and [M([18]ane-N_6)]$(TCNQ)_4$, depending on the use of radical-anionic or mixed-valence TCNQ salts in the reaction. The crystal structures of the nickel derivatives show that the former derivatives are built up by macrocyclic metal cations surrounded by dimeric dianions $(TCNQ)_2^{2-}$, either isolated or stacked along the crystal. The derivative with four TCNQ units/formula consists of alternated chains of metallomacrocyclic cations and stacked TCNQ anions. The crystal parameters suggest that every TCNQ holds approximately 0.5 electrons and overlaps with a neighboring unit to form dimeric monoanions, $(TCNQ)_2^-$.

Introduction

There is considerable interest in the chemistry of polyazamacrocycles because of their ability to act as models for molecular recognition in protein sites.[1] Large cyclic polyamines, with six or more donor atoms, have the adequate size and flexibility to form stable complexes by encapsulating the metal ion in an octahedral environment.[2] These macrocycles can be also protonated to form polyammonium cations which give rise to strong interactions with anions.[3]

The six-nitrogen-containing macrocycle 1,4,7,10,13,16-hexaazacyclooctadecane, [18]ane-N_6, can coordinate in an octahedral way large metal ions such as mercury(II),[4] cobalt-(III),[5] or chromium(III).[6] The big size cavity of this macrocycle can also host two smaller metal ions as observed in acetate and phosphate dicopper derivatives.[7]

* To whom correspondence should be addressed. E-mail: alonso@quim.ucm.es.
[†] Universidad Complutense.
[‡] Academy of Science of Moldova.
[§] Adam Mickiewicz University.

(1) (a) Mertes, K. B.; Lehn, J. M. In *Comprehensive Coordination Chemistry*; Wilkinson, G., Ed.; Pergamon: Oxford, U.K., 1987; p 915. (b) Lindoy, L. F. *The Chemistry of Macrocyclic Ligand Complexes*; Cambridge University Press: Cambridge, U.K., 1989. (c) Lehn, J. M. *Supramol. Chem.* VCH: Weinheim, Germany, 1995.
(2) (a) Bencini, A.; Bianchi, A.; Paoletti, P.; Paoli, P. *Coord. Chem. Rev.* **1992**, *120*, 51−85. (b) Mitewa, M.; Bontchev, P. R. *Coord. Chem. Rev.* **1994**, *135/136*, 129−163.
(3) (a) Cullinane, J.; Gelb, R. I.; Margullis, T. N.; Zompa, L. J. *J. Am. Chem. Soc.* **1982**, *104*, 3048−3053. (b) Kimura, E.; Kodama, M.; Yatsunami, T. *J. Am. Chem. Soc.* **1982**, *104*, 3182−3187. (c) Hosseini, M. W.; Lehn, J. M. *J. Am. Chem. Soc.* **1982**, *104*, 3525−3527. (d) Mosier-Boss, P. A.; Popov, A. I. *J. Am. Chem. Soc.* **1985**, *107*, 6168−6174. (e) Santos, M. A.; Drew, M. G. B. *J. Chem. Soc. Faraday Trans.* **1991**, *87*, 1321−1331.
(4) Carrondo, M. A. A. F.; Felix, V.; Duarte, M. T.; Santos, M. A. *Poyhedron* **1993**, *12*, 931−937.
(5) Royer, D. J.; Grant, G. J.; VanDerveer, D. G.; Castillo, M. J. *Inorg. Chem.* **1982**, *21*, 1902−1908.
(6) Chandrasekhar, S.; Fortier, D. G.; McAuley, A. *Inorg. Chem.* **1993**, *32*, 1424−1429.

10.1021/ic062016h CCC: $37.00
Published on Web 04/19/2007

In the past years we have been interested in the study of the reactivity of TCNQ polynitrile radicals toward nickel and copper macrocyclic complexes and in the determination of the influence of the metal environment in the final supramolecular structure. The two main factors involved are the metal environment and the formal oxidation state of the TCNQ. The former determines the ability of the metal atom to form σ bonds with the radical TCNQ, a fact usually observed when the metal has free positions in their coordination environment.[8] On the contrary, with fully coordinated metals the supramolecular species formed show no direct bonding interactions between the metal and the TCNQ.[9] The TCNQ oxidation state also affects the supramolecular architecture since the fully reduced radical $TCNQ^-$ shows higher coordinative ability and tends to form diamagnetic dimers, $(TCNQ)_2^{2-}$,[8,9] while when TCNQ is partially reduced, a greater delocalization along the formation of stacks and no direct interaction with the metal are observed.[9,10]

Surprisingly the degree of TCNQ reduction and then the delocalization seems to be regulated by the size of the metal complex acting as counterion since the positive charges must be neutralized by the TCNQ stacks. Depending on the cation, the equivalent volume in the stack is occupied by two, three, or four TCNQ units; with a dipositive cation it means that every TCNQ bears 1, 0.66, or 0.5 electrons, respectively.[10] To check this fact with new examples, we have planned the study of the derivatives formed by interaction of fully or partially reduced TCNQ salts with complexes of nickel and copper coordinated to the big size macrocycle [18]ane-N_6. The main results are reported in this work.

Experimental Section

All the reactions have been carried out under oxygen-free nitrogen using the starting materials as purchased.

[Ni([18]ane-N_6)]$(NO_3)_2$ (1). A solution containing 0.26 g (1 mmol) of [18]ane-N_6 in 15 mL of methanol was added over a solution of 0.29 g (1 mmol) of $Ni(NO_3)_2{\cdot}6H_2O$ in 15 mL of methanol. After 5 h of stirring, a pink solid appeared, which was filtered off, washed with methanol and diethyl ether, and dried under vacuum. Yield: 72%. Anal. Calcd for $C_{12}H_{30}N_8NiO_6$: C, 32.7; H, 6.7; N, 25.4. Found: C, 32.9; H, 6.3; N, 25.3. IR data (KBr, cm^{-1}): 3410 m, 3210 s, 2935 s, 2872 s, 1742 w, 1461 m, 1346 s, 1137 m, 1098 m, 1062 m, 1027 w, 1005 w, 958 s, 840 m, 652 w, 610 w, 512 w, 406 m.

[Cu_2([18]ane-N_6)Cl_2]$Cl_2{\cdot}4H_2O$ (2). To a solution of 0.34 g (2 mmol) of $CuCl_2{\cdot}2H_2O$ in 15 mL of methanol was added 0.26 g (1 mmol) of [18]ane-N_6 dissolved in 15 mL of methanol. After a few minutes of stirring, a blue solid appeared which was filtered off, washed with methanol and diethyl ether, and dried under vacuum. Yield: 54%. Anal. Calcd for $C_{12}H_{38}Cl_4Cu_2N_6O_4$: C, 24.1; H, 6.4; N, 14.0. Found: C, 24.4; H, 6.1; N, 14.2. IR data (KBr, cm^{-1}): 3407 s, 3150 s, 2968 m, 2937 m, 2870 m, 1641 w, 1515 w, 1468 m, 1454 m, 1439 m, 1373 w, 1343 w, 1331 w, 1316 w, 1297 w, 1255 w, 1139 w, 1115 w, 1092 w, 1060 m, 1040 s, 1024 s, 945 m, 900 w, 845 w, 724 m, 651 m, 561 w, 511 w, 447 w.

[Cu([18]ane-N_6)]$Cl_2{\cdot}H_2O$ (3). A solution containing 0.26 g (1 mmol) of [18]ane-N_6 in 15 mL of methanol was added over a solution of 0.17 g (1 mmol) of $CuCl_2{\cdot}2H_2O$ in 15 mL of methanol. After 6 h of stirring, a blue solid, identified as **2**, appeared and was filtered off. The solution was cooled overnight, and the blue crystals which formed were filtered off and dried in air. Yield: 32%. Anal. Calcd for $C_{12}H_{32}Cl_2CuN_6O$: C, 35.1; H, 7.9; N, 20.4. Found: C, 35.5; H, 7.9; N, 20.6. IR data (KBr, cm^{-1}): 3490 s, 3405 m, 3160 s, 3110 s, 2936 s, 2870 m, 1612 m, 1470 s, 1454 m, 1420 m, 1373 w, 1346 m, 1308 w, 1255 w, 1142 w, 1100 s, 1082 w, 986 m, 937 m, 856 w, 790 m, 769 w, 460 m.

[Ni([18]ane-N_6)]$(TCNQ)_2$ (4). A solution containing 0.32 g (1.5 mmol) of LiTCNQ in 15 mL of methanol was dropwise added over a stirred solution containing 0.33 g (0.75 mmol) of **1** in a mixture of methanol (15 mL)/water (5 mL). After complete mixing, a blue solid appeared, which was filtered off, washed with methanol, and dried under vacuum. Yield: 67%. Anal. Calcd for $C_{36}H_{38}N_{14}Ni$: C, 59.6; H, 5.3; N, 27.0. Found: C, 59.3; H, 5.0; N, 26.8. IR data (KBr, cm^{-1}): 3440 m, 3280 m, 2877 w, 2181 s, 2157 s, 1581 m, 1505 m, 1348 m, 1177 m, 988 w, 955 w, 822 w, 718 w, 541 w, 478 w.

[Cu([18]ane-N_6)]$(TCNQ)_2$ (5). Compound **5** was synthesized by a procedure similar to that for **4**, using **3** as starting material. Yield: 45%. This compound has also been prepared by the same procedure starting from **2** and LiTCNQ in a molar ratio 1:1 with a 31% yield. Anal. Calcd for $C_{36}H_{38}CuN_{14}$: C, 59.2; H, 5.2; N, 26.8. Found: C, 59.3; H, 5.0; N, 26.5. IR data (KBr, cm^{-1}): 3201 m, 2944 w, 2186 s, 2176 s, 2161 m, 1583 m, 1505 m, 1432 w, 1365 m, 1348 m, 1179 m, 1092 w, 1027 w, 988 w, 825 w, 720 w, 479 w.

[Ni([18]ane-N_6)]$(TCNQ)_4$ (6). A solution containing 0.66 g (1.3 mmol) of $(NEt_3H)(TCNQ)_2$ in 20 mL of acetonitrile was dropwise added over a stirred solution of 0.29 g (0.65 mmol) of **1** in a mixture of methanol (15 mL)/water (5 mL). After complete mixing a dark blue solid appeared, which was filtered off, washed with methanol, and dried under vacuum. Yield: 51%. Anal. Calcd for $C_{60}H_{46}N_{22}$-Ni: C, 63.6; H, 4.1; N, 27.2. Found: C, 63.4; H, 4.1; N, 26.6. IR data (KBr, cm^{-1}): 3480 w, 3270 w, 2163 s, 1567 s, 1507 m, 1478 w, 1334 s, 1162 s, 1087 w, 949 m, 835 w, 789 w, 700 m, 609 w, 483 w.

[Cu([18]ane-N_6)]$(TCNQ)_4$ (7). This compound was synthesized from derivative **3** by a procedure similar to that described for **6**. Yield: 43%. Anal. Calcd for $C_{60}H_{46}CuN_{22}$: C, 63.3; H, 4.1; N, 27.1. Found: C, 62.8; H, 4.3; N, 27.1. IR data (KBr, cm^{-1}): 3460 w, 3250 w, 2199 s, 2171 m, 1574 m, 1506 s, 1353 m, 1328 m, 1223 w, 1179 m, 1012 w, 990 w, 832 w, 799 w, 696 w, 483 w.

(7) Barker, J. E.; Liu, Yu; Martin, D. N.; Ren, T. *J. Am. Chem. Soc.* **2003**, *125*, 13332−13333.

(8) (a) Cornelissen, J. P.; Diemen, J. H.; Groenveld, L. R.; Hasnoot, J. G.; Speck, A. L.; Reedijk, R. J. *Inorg. Chem.* **1992**, *31*, 198−202. (b) Ballester, L.; Barral, M. C.; Gutiérrez, A.; Monge, A.; Perpiñán, M. F.; Ruiz Valero, C.; Sanchez Pélaez, A. *Inorg. Chem.* **1994**, *33*, 2142−2146. (c) Kunkeler, P.; Koningsbruggen, P. J.; Cornelissen, J. P.; van der Horst, A. N.; van del Kraan, A. M.; Spek, A. L.; Haasnoot, J. A.; Reedijk, J. *J. Am. Chem. Soc.* **1996**, *118*, 2190−2197. (d) Ballester, L.; Gutiérrez, A.; Perpiñán, M. F.; Amador, U.; Azcondo, M. T.; Sánchez-Peláez, A. E.; Bellitto, C. *Inorg. Chem.* **1997**, *36*, 6390−6396. (e) Choi, H. J.; Myunghyun, P. S. *Inorg. Chem.* **2003**, *42*, 1151−1157.

(9) (a) Azcondo, M. T.; Ballester, L.; Golhen, S.; Gutiérrez, A.; Ouahab, L.; Yartsev, S.; Delhaes, P. *J. Mater. Chem.* **1999**, *9*, 1237−1244. (b) Ballester, L.; Gil, A. M.; Gutiérrez, A.; Perpiñán, M. F.; Azcondo, M. T.; Sánchez-Peláez, A. E.; Coronado, E.; Gómez-García, C. J. *Inorg. Chem.* **2000**, *39*, 2837−2842. (c) Alonso, C.; Ballester, L.; Gutiérrez, A.; Perpiñán, M. F.; Sánchez, A. E.; Azcondo, M. T. *Eur. J. Inorg. Chem.* **2005**, 486−495.

(10) (a) Ballester, L.; Gutiérrez, A.; Perpiñán, M. F.; Rico, S.; Azcondo, M. T.; Bellitto, C. *Inorg. Chem.* **1999**, *38*, 4430−4434. (b) Ballester, L.; Gil, A. M.; Gutiérrez, A.; Perpiñán, M. F.; Azcondo, M. T.; Sánchez-Peláez, A. E.; Marzin, C.; Tarrago, G.; Bellitto, C. *Chem.—Eur. J.* **2002**, *8*, 2539−2548.

Table 1. Crystallographic Data for Compounds **2**−**4** and **6**

param	**2**	**3**	**4**	**6**
formula	$C_{12}H_{38}Cl_4Cu_2N_6O_4$	$C_{12}H_{32}Cl_2CuN_6O$	$C_{36}H_{38}N_{14}Ni$	$C_{60}H_{46}N_{22}Ni$
fw	599.36	410.88	725.51	1133.90
T (K)	296	293	293	160
cryst syst	monoclinic	monoclinic	triclinic	triclinic
space group (No.)	$C2/m$ (12)	$P2_1/n$ (14)	$P\bar{1}$ (2)	$P\bar{1}$ (2)
a (Å)	12.4550(14)	13.1690(12)	15.349(3)	8.805(2)
b (Å)	15.6884(17)	9.3466(9)	15.598(3)	12.308(2)
c (Å)	6.2507(7)	15.2323(14)	16.174(3)	13.052(3)
α (deg)	90	90	75.769(4)	78.04(3)
β (deg)	90.806(2)	97.627(2)	75.452(5)	86.39(3)
γ (deg)	90	90	85.635(4)	76.43(3)
V (Å^3)	1221.3(2)	1858.3(3)	3632.6(11)	1345.0(5)
Z	2	4	4	1
ρ_{calcd} (g cm^{-3})	1.630	1.469	1.327	1.400
μ (mm^{-1})	2.208	1.473	0.582	0.425
R1[a]	0.0239	0.0432	0.0506	0.0578
wR2[b]	0.0667	0.0960	0.1598	0.1787

[a] $R1 = \Sigma||F_o| - |F_c||/\Sigma|F_o|$. [b] $wR2 = \{\Sigma[w(F_o^2 - F_c^2)^2]/\Sigma[w(F_o^2)^2]\}^{1/2}$.

Physical Measurements. Elemental analyses were carried out by the Servicio de Microanálisis of the Universidad Complutense de Madrid. Infrared spectra were recorded as KBr pellets on a Nicolet Magna-550 FT-IR spectrophotometer. Electronic spectra were recorded using a Cary-5 spectrophotometer. The spectra were recorded in the solid state. The solid samples were prepared by rubbering the sample on optical glass. Magnetic experiments were made on polycrystalline samples using a SQUID magnetometer MPMS-XL-5 manufactured by Quantum Design. The temperature dependence of the magnetization in the range between 2 and 300 K was recorded using a constant magnetic field of 0.5 T. The experimental data have been corrected for the magnetization of the sample holder (gelatine) and for atomic diamagnetism as calculated from the known Pascal's constants. Electrical conductivity measurements at room temperature were performed by the two points method in pressed powdered samples.[11]

Crystallographic Studies. Good quality crystals of **2**−**4** and **6** were obtained by slow diffusion of diluted solutions of the reactants. A summary of the fundamental crystal data is given in Table 1. For **2**−**4**, the crystal data were collected in the "CAI de Difracción de Rayos X, UCM". In all the cases a blue crystal was resin epoxy coated and mounted on a Bruker Smart CCD diffractrometer using graphite-monochromated Mo Kα radiation (λ = 0.710 73 Å) operating at 50 kV and 25 mA. Data were collected over a reciprocal space hemisphere by combination of three exposure sets. Each frame exposure time was 20 s covering 0.3° in ω. The cell parameters were determined and refined by least-squares fit of all reflections collected. The first 50 frames were recollected at the end of the data collection to monitor crystal decay, and no appreciable decay was observed. Crystal data for **6** were collected at 160 K on a KUMA KM4CCD diffractometer using graphite-monochromated Mo Kα radiation (λ = 0.710 73 Å) operating at 50 kV and 40.0 mA. A dark-red colored crystal was selected for the measurements. The reflection intensities were collected from 100 frames. The exposure time/frame was 18 s. The results were processed using the Kuma Diffraction software (Wroclaw, Poland). No absorption correction was applied. All the structures were solved by direct methods and refined by applying full-matrix least-squares on F^2 with anisotropic thermal parameters for the non-hydrogen atoms. The hydrogen atoms were included with fixed isotropic contributions at their calculated positions determined by molecular geometry, except for the water molecules in **2** and **3** whose hydrogen atoms were located from the Fourier map and refined riding on the corresponding oxygen. The refinement of **4** affords high thermal parameters for the majority of the carbon and nitrogen atoms giving final poor results; this fact should be related with the poor quality of the starting data (R_{int} = 0.25). All the calculations were carried out with the SHELX97 software package.[12]

Results and Discussion

The reaction of [18]ane-N_6 with $CuCl_2 \cdot 2H_2O$ affords two different products, **2** and **3**, depending on the reaction conditions. After immediate mixing of the reagents, the dinuclear derivative **2** appears as a solid. When the reaction is left stirring for a prolonged time, the mononuclear compound **3** is formed. Compound **2** can be directly isolated in good yields using a 1:2 macrocycle to copper molar ratio and short reaction times, but for compound **3** we have always obtained different quantities of **2** as a byproduct; the best yields of the former were obtained using the conditions described in the Experimental Section. The reaction to get the corresponding nickel derivative always lead to the mononuclear species **1**, due to the use of nitrate as anion, less prone to behave as a bridging ligand than the chloride. No pure compounds were isolated from the reaction between [18]ane-N_6 and $NiCl_2 \cdot 6H_2O$.

These reagents react with TCNQ salts with displacement of the anions and formation of the corresponding TCNQ derivatives, **4**−**7**. In the reactions with LiTCNQ only the radical anion is present, and since the obtained derivatives, **4** and **5**, show the general formula [M([18]ane-N_6)](TCNQ)$_2$, no significant charge transfer takes place during the reaction. It should be noted that the dinuclear copper derivative **2** reacts with LiTCNQ with formation of the mononuclear species, **5**. From the reaction mixture the compound [Cu(TCNQ)$_2$]$\cdot H_2O$ has been identified by its IR spectrum, indicating that the reaction stoichiometry is

(11) Wudl, F.; Brice, M. R. *J. Chem. Educ.* **1990**, *67*, 717−718.

(12) Sheldrichk, G. M. *SHELX-97*; University of Göttingen: Göttingen, Germany, 1997.

$$[Cu_2([18]ane\text{-}N_6)Cl_2]Cl_2{\cdot}4H_2O + 4LiTCNQ \rightarrow [Cu([18]ane\text{-}N_6)](TCNQ)_2 + [Cu(TCNQ)_2]{\cdot}H_2O + 4LiCl$$

The unstability of the dinuclear Cu_2Cl_2 moiety in this reaction can indicate that it occurs with a nucleophilic attack of the radical anion $TCNQ^-$ over the copper atom.

When $(NEt_3H)(TCNQ)_2$ is used as the reacting agent, the derivatives of formula $[M([18]ane\text{-}N_6)](TCNQ)_4$, **6** and **7**, are obtained. The reactions again correspond to an anion metathesis since the formal oxidation state, $TCNQ^{0.5-}$, expected for these compounds is the same as in the starting ammonium salt.

IR Spectra and Electrical Conductivity. The IR spectra of the studied derivatives show the typical features found in other uncoordinated TCNQ compounds.[13] The most significant bands for the anionic TCNQ are the ν(CN) = 2194/2157 cm^{-1}, $\nu_{20}(b_{1u}) = 1507$ cm^{-1}, and $\nu_{50}(b_{3u}) = 824$ cm^{-1}; these bands are shifted to higher frequencies on reducing the electronic charge on the TCNQ. Compounds **4** and **5** show these bands with typical values for uncoordinated dimeric $(TCNQ)_2^{2-}$ anions,[8] in consonance with a model of cationic $[M([18]ane\text{-}N_6)]^{2+}$ and anionic $(TCNQ)_2^{2-}$ alternating in the structure, as commented below. This picture is always associated with localized electronic charges leading to very low conductivity values. In fact, the room-temperature conductivity measurements for **4** and **5** gave values well below 10^{-7} S cm^{-1}.

The spectra of **6** and **7** show very different features, with bands at 2199−2163, 1507, and 835−832 cm^{-1} for the TCNQ significant vibrational modes. The frequency values, especially the ν_{50} band, are intermediate between the usual values of the neutral and mononegative TCNQ, suggesting that the acceptor has a formally nonintegral oxidation state. More noticeable is the fact that all these bands appear superimposed on a low-energy electronic absorption centered at 3180 cm^{-1} for compound **6** and at 3960 cm^{-1} for **7** and is attributed to a charge-transfer band (CT_2) between adjacent radical anionic and neutral TCNQ groups, a typical feature of the presence of partially reduced TCNQ stacks showing some degree of electronic delocalization.[14] These compounds usually show a semiconducting behavior as observed by the room-temperature values of the electrical conductivity of **6**, 7.7×10^{-4} S cm^{-1}, and **7**, 3.1×10^{-4} S cm^{-1}. These values correspond to weak semiconductors and are similar to those found in other stacks of $TCNQ^{0.5-}$.[9c,10a]

Crystal Structure of 2. This compound crystallizes in the *C*2/*m* monoclinic group. Figure 1 shows an ORTEP view of the compound with the labeling scheme of the asymmetric unit. The formula unit consists of one macrocyclic cation, $[Cu_2([18]ane\text{-}N_6)Cl_2]^{2+}$, two chloride anions, and four water molecules. The complex cation possesses a 2/*m* symmetry

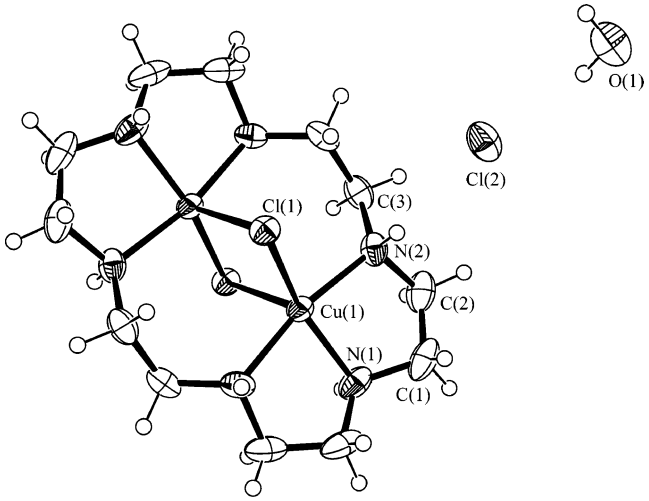

Figure 1. ORTEP view, 50% probability ellipsoids, of $[Cu_2([18]ane\text{-}N_6)Cl_2]Cl_2{\cdot}4H_2O$ (**2**). Selected bond lengths (Å) and angles (deg): Cu1−N1, 2.008(3); Cu1−N2, 2.036(2); Cu1−Cl1, 2.318(1); Cu1−Cl1′, 2.591(1); Cl2−O1, 3.180(8); Cl2−N2, 3.302(2); O1−O1′, 2.733(9); N1−Cu1−N2, 84.99(6); N2−Cu1−N2, 168.88(12); N1−Cu1−Cl1, 154.46(10); N1−Cu1−Cl1′, 102.23(9); N2−Cu1−Cl1, 93.48(6); Cl1−Cu1−Cl1′, 103.31(3).

and is formed by a central Cu_2Cl_2 core surrounded by the [18]ane-N_6 macrocycle which coordinates the two copper atoms; the copper atoms are five-coordinated to three nitrogen atoms corresponding to half of the macrocycle and to the two bridging chlorine atoms. The type of environment can be determined by means of the Addison parameter, which measures the degree of trigonality in a five-coordinated environment,[15] ranging from $\tau = 0$, for a perfect square planar environment, to $\tau = 1$, for the perfect trigonal bipyramid. In compound **2** the Addison parameter has a value of $\tau = 0.24$ indicating a distorted square pyramidal environment for the copper atoms, with three nitrogen atoms and one bridging chlorine in the basal plane and the other chlorine atom in apical position. The copper atom is located 0.30 Å above the pyramid basal plane. The copper−chlorine distances are different, the larger distance corresponding to the apical chlorine, a situation frequently found in related Cu_2Cl_2 moieties.[16] These macrocyclic cations are stacked along the crystal *c*-axis leaving channels occupied by the chloride anions and the water molecules which, in turn, are linked through hydrogen bonds forming infinite chains, as shown in Figure 2. The chlorine atom forms two equivalent hydrogen bonds with symmetry-related water molecules; the bond parameters are O1−H01A = 0.87 Å, H01A···Cl2 = 2.36 Å, and angle O1−H01A−Cl2 = 157°. The water molecules are also hydrogen bonded in a rectangular shape with distances $O1\cdots O1(x, -y, z) = 2.73$ Å and $O1\cdots O1(1 - x, y, 2 - z) = 2.80$ Å.

These chains are linked to the macrocycles through extra hydrogen bonds; two are formed between each Cl2 and the amine groups of two adjacent macrocycles and extend the

(13) (a) Bozio, R.; Girlando, A.; Pecile, C. *J. Chem. Soc., Faraday Trans.* **1975**, *71*, 1237−1254. (b) Bozio, R.; Zanon, I.; Girlando, A.; Pecile, C. *J. Chem. Soc., Faraday Trans. 2* **1978**, *74*, 235−248. (c) Ballester, L.; Gutiérrez, A.; Perpiñán, M. F.; Azcondo, M. T. *Coord. Chem. Rev.* **1999**, *190*−*192*, 447−470.

(14) (a) Inoue, M.; Inoue, M. B. *J. Chem. Soc., Faraday Trans.* **1985**, *81*, 539−547. (b) Ghezzal, E.; Brau, A.; Farges, J. P.; Dupuis, P. *Mol. Cryst. Liq. Cryst.* **1992**, *211*, 327−330.

(15) Addison, A. W.; Rao, T. N.; Reedijk, J.; van Rijn, J.; Verschoor, G. C. *J. Chem. Soc., Dalton Trans.* **1984**, 1349−1356.

(16) (a) Puschmann, H.; Batsanov, A. S.; Howard, J. A. K.; Soto, B.; Bonne, R.; Au-Alvarez, O. *Acta Crystallogr., Sect E* **2001**, *E57*, m524−m526. (b) Halfen, J. A.; Fox, D. C.; Mehn, M. P.; Que, L. *Inorg. Chem.* **2001**, *40*, 5060−5061. (c) Weghorn, S. J.; Sessler, J. L.; Lynch, V.; Baumann, T. F.; Sibert, J. W. *Inorg. Chem.* **1996**, *35*, 1089−1090.

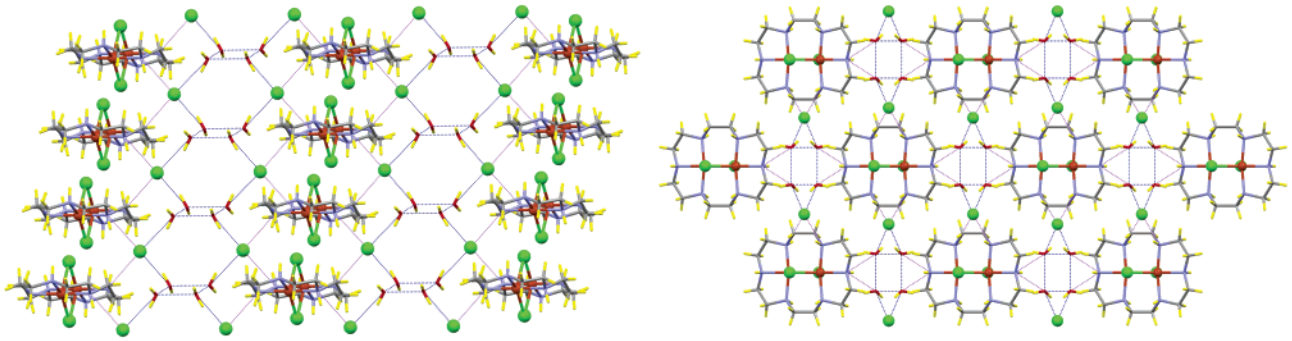

Figure 2. Two views of the packing of **2** showing the hydrogen bonds formed between the chloride anions and the crystallization water molecules as blue dotted lines and those implying the macrocyclic nitrogens as purple dotted lines.

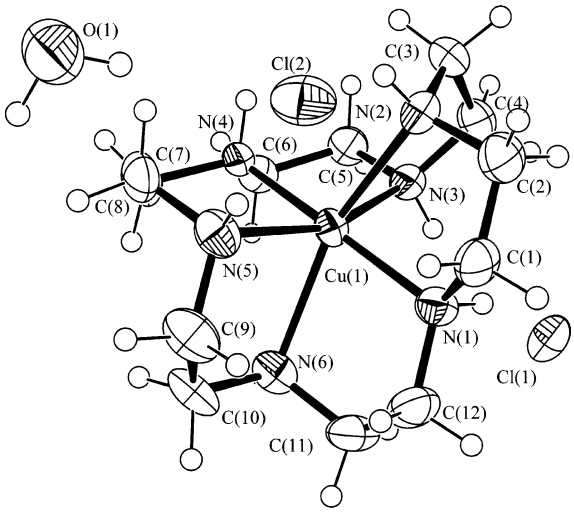

Figure 3. ORTEP view, 50% probability ellipsoids, of [Cu([18]ane-N_6)]-Cl_2·H_2O (**3**). Selected bond lengths (Å): Cu1−N1, 2.043(3); Cu1−N2, 2.290(3); Cu1−N3, 2.175(3); Cu1−N4, 2.002(3); Cu1−N5, 2.189(3); Cu1−N6, 2.318(3).

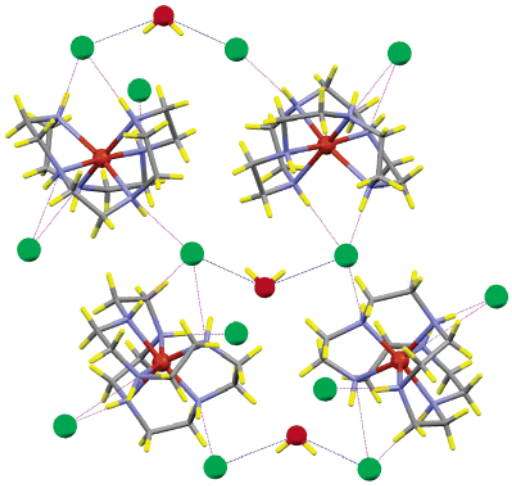

Figure 4. Packing view of **3**. The hydrogen bonds are shown as dotted lines. Bond distances (Å) and angles (deg): O1−H01 = 0.98, H01···Cl1 = 2.35, O1−H01−Cl1 = 153; O2−H02 = 0.91, H02···Cl2 = 2.43, O1−H02−Cl2 = 145; N1−H1 = 0.91, H1···Cl1 = 2.61, N1−H1−Cl1 = 154; N2−H2 = 0.910, H2···Cl2 = 2.73, N2−H2−Cl2 = 134; N3−H3 = 0.91, H3···Cl1 = 2.49, N3−H3−Cl1 = 149; N4−H4 = 0.91 Å, H4···Cl2($-x$ + 1/2, y − 1/2, $-z$ + 3/2) = 2.36, N4−H4−Cl2 = 158; N5−H5 = 0.91, H5···Cl2 = 2.38, N5−H5−Cl2 = 171; N6−H6 = 0.91, H6···Cl1($-x$ + 3/2, y − 1/2, $-z$ + 3/2) = 2.37, N6−H6−Cl1 = 162.

intermolecular interactions along the *b* crystal axis: N2−H2 = 0.91 Å; H2···Cl2 = 2.54 Å; angle N2−H2−Cl2 = 142°. Finally, the water molecules form hydrogen bonds with the macrocyclic nitrogen not bound to the chlorine atoms, N1−H1 = 0.91 Å, H1···O1 = 2.65 Å, and angle N1−H1−O1 = 144°, along the *a* crystal axis completing the net of hydrogen bonds linking the different molecules in the crystal.

Crystal Structure of 3. This compound crystallizes in the monoclinic $P2_1/n$ group. The asymmetric unit is shown in Figure 3 and consists of one metallomacrocyclic cation, two chloride anions, and one water molecule.

The copper atom is octahedrically coordinated to the six nitrogen atoms in the macrocycle. Both facial[17] and meridional[18] isomers have been found in coordination complexes. Compound **3** corresponds to the *mer* isomer. The Cu−N bond distances indicate a rhombic distortion in the octahedron with opposite distances of ca. 2.0, 2.2, and 2.3 Å, respectively; the shortest Cu−N distances are due to the meridional nitrogen atoms. Due to this rhombic distortion, the two meridional planes intersect with an angle of 78.8°, with the copper atom slightly displaced (0.040 and 0.043 Å) from these planes.

Figure 4 shows that the chlorine atoms and the crystallization water molecule are linking the metallomacrocycles through a series of hydrogen bonds involving the six amine groups of every macrocycle. The water molecule form two hydrogen bonds with the chlorine atoms; the Cl1···O1···Cl2 unit forms an angle of 127° and is surrounded by four macrocyclic cations that form hydrogen bonds with the chlorine atoms. Every macrocycle is linked to four chlorine atoms since two of them are doubly bonded, forming, as in the previous structure, a three-dimensional network of hydrogen bonds that supports the structure.

Crystal Structure of 4. This compound crystallizes in the triclinic $P\bar{1}$ group. The asymmetric unit consists of two metallomacrocyclic cations and four TCNQ radical anions. Their ORTEP view is shown in Figure 5.

The nickel atoms in both cations are six-coordinated by the nitrogen atoms of the macrocycle, which forms the meridional isomer as in **3** but with a less distorted coordinative environment. The Ni−N distances are shorter for the

(17) (a) Searle, G. H.; Tiekink, E. R. *J. Coord. Chem.* **1989**, *20*, 229−235. (b) Chandrasekhar, S.; Fortier, D. G.; McAuley, A. *Inorg. Chem.* **1993**, *32*, 1424−1429.

(18) (a) Yodhikawa, Y. *Bull. Chem. Soc. Jpn.* **1982**, *55*, 412. (b) Royer, D. J.; Grant, G. J.; Van Derveer, D. G.; Castillo, M. J. *Inorg. Chem.* **1982**, *21*, 1902−1908.

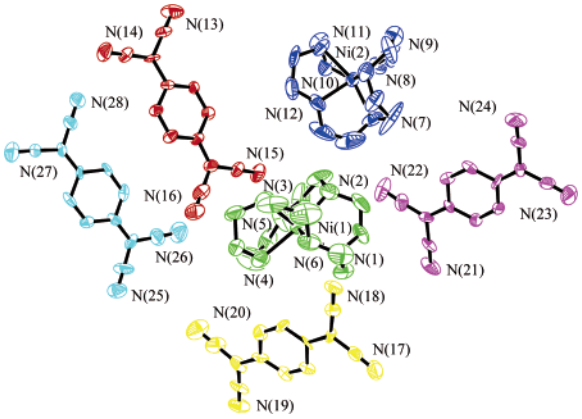

Figure 5. ORTEP view, 50% probability ellipsoids, of [Ni([18]ane-N_6)]-$(TCNQ)_2$ (**4**), showing the labeling of nitrogen and nickel atoms. The color pattern corresponds to that described in the text: TCNQ A, red; TCNQ B, cyan; TCNQ C, yellow; TCNQ D, magenta.

Table 2. Hydrogen Bonds Found in the Crystal Structure of Compounds **4** and **6**

compd	D−H···A	*d*(D−H), Å	*d*(H···A), Å	angle, deg
4	N1−H1···N18 (TCNQ C)	0.91	2.32	158
	N2−H2···N25 (TCNQ B)	0.91	2.21	159
	N4−H4···N21(TCNQ D)	0.91	2.31	140
	N6−H6···N13 (TCNQ A)	0.91	2.11	164
	N7−H7···N14 (TCNQ A)	0.91	2.28	149
	N8−H8···N24 (TCNQ D)	0.91	2.35	138
	N10−H10···N15 (TCNQ A)	0.91	2.22	161
	N11−H11···N19 (TCNQ C)	0.91	2.32	148
	N12−H12···N27 (TCNQ B)	0.91	2.43	160
6	N1−H1···N3A	0.84	2.68	126
	N4−H4···N3A	0.93	2.40	139
	N7−H7···N3B	0.92	2.43	142

meridional nitrogen atoms (N3, N6, N9, N12), ranging between 2.04(1) and 2.07(1) Å. The other Ni−N distances are in the range 2.12(1)−2.16(1) Å giving a flattened octahedral environment for the nickel atoms.

The four TCNQ of the asymmetric unit are crystallographically different and have been identified by us with the labels A−D. All the TCNQ must be anion-radicals, as the IR spectrum suggests, since four negative charges are needed to neutralize the two macrocyclic cations; however, the poor quality of the data precludes a confirmation on the basis of the interatomic distances in the TCNQ species.

The crystal packing (Figure 6) can be described as a bidimensional array of noninteracting metallomacrocyclic cations stacked along the [010] and [10$\bar{1}$] directions. The TCNQ units are located between the macrocyclic sheets forming dimeric dianions that stack in two different ways. TCNQ A and B form infinite stacks along the [010] crystal direction. The stack is built up of π overlapping TCNQ units in the sequence ···B−A−A−B−B−A··· with shortest intradimer distances of 3.16 Å (A−A) and 3.47 Å (B−B) and an interdimer (A−B) distance of 3.20 Å. TCNQ A and B are not strictly parallel but form an angle of 7° between their ring planes. Alternatively, the stack can be described as formed by π overlapping tetramers B−A−A−B with short contacts inside the tetramer and longer distances in between. TCNQ C and D form dimers (C−D) in the [10$\bar{1}$] direction, with an interplanar distance of 3.25 Å. Two of the dimers are stacked in the sequence D−C−C−D, but the interdimer (C−C) distance of 3.62 Å is too long to consider the presence of π interactions between the dimers. These TCNQ are perpendicular to the stack of TCNQ A and B and along with the metallomacrocycles surround the channels where these stacks are located. The intermolecular interactions in this crystal are completed by hydrogen bonds between the amine groups of the macrocycles and cyano groups in the TCNQ units; these bonds are listed in Table 2.

Crystal Structure of 6. This compound crystallizes in the triclinic $P\bar{1}$ group. The asymmetric unit is shown in Figure 7 and consists of half of the metallomacrocyclic cation and two TCNQ anions.

The nickel is octahedrically coordinated by the six nitrogen atoms of the macrocycle. In contrast to the previous examples, the metallomacrocyclic cation forms the less common facial isomer.[17] The coordination environment is highly regular with the six Ni−N distances equal within the experimental error: Ni1−N1 = 2.157(2) Å; Ni1−N4 = 2.155(2) Å; Ni1−N7 = 2.154(2) Å.

The two crystallographically independent TCNQ molecules are labeled A and B. According to the relation between carbon−carbon bond distances and the negative charge located on the organic acceptor,[19] both TCNQ show similar parameters (Table 3) and, within experimental error, they correspond to a formal charge of 0.5 electron. All the TCNQ species are stacked along the [100] direction interacting by π overlap with neighboring units (Figure 8). TCNQ A and B alternate along the stack with shortest distances of 3.15 and 3.30 Å. According to the lack of uniformity indicated by these intermolecular distances, the stack can be alternatively seen as overlapping $(TCNQ)_2^-$ dimers showing stronger interactions inside the dimer.

As in the previous structure, the electrostatic interactions between the metallomacrocyclic cations and the TCNQ anionic stack are complemented by the formation of several hydrogen bonds between the amine macrocyclic groups and the TCNQ cyano groups (Table 2).

Magnetic Properties. The magnetic susceptibilities of **1**−**7** have been measured in the temperature range 2−300 K.

The magnetic moments of the nickel derivatives **1** and **4** follow the Curie law above 20 K, arising only from isolated nickel(II), $S = 1$, spins. Below this temperature, there is an abrupt descent in the moment values and this fact can be ascribed to the presence of a zero-field splitting in the ground state, which is one of the most important sources of magnetic anisotropy in nickel(II) octahedral derivatives.[21] Equation 1 takes into account this single-ion anisotropy for the average magnetic susceptibility, where g_{Ni} is the Landé g factor for

(19) Kistenmacher, T. J.; Emge, T. J.; Bloch, A. N.; Cowan, D. O. *Acta Crystallogr., Sect. B* **1982**, *38*, 1193−1199.
(20) Goldberg, S. Z.; Eisenber, R.; Miller, J. S.; Epstein, J. A. *J. Am. Chem. Soc.* **1976**, *98*, 5173−5182 and references therein.
(21) (a) Carlin, R. L. *Magnetochemistry*; Springer-Verlag: Berlin, 1986; p 24. (b) Kahn, O. *Molecular Magnetism*; VCH: New York, 1993; p 17.

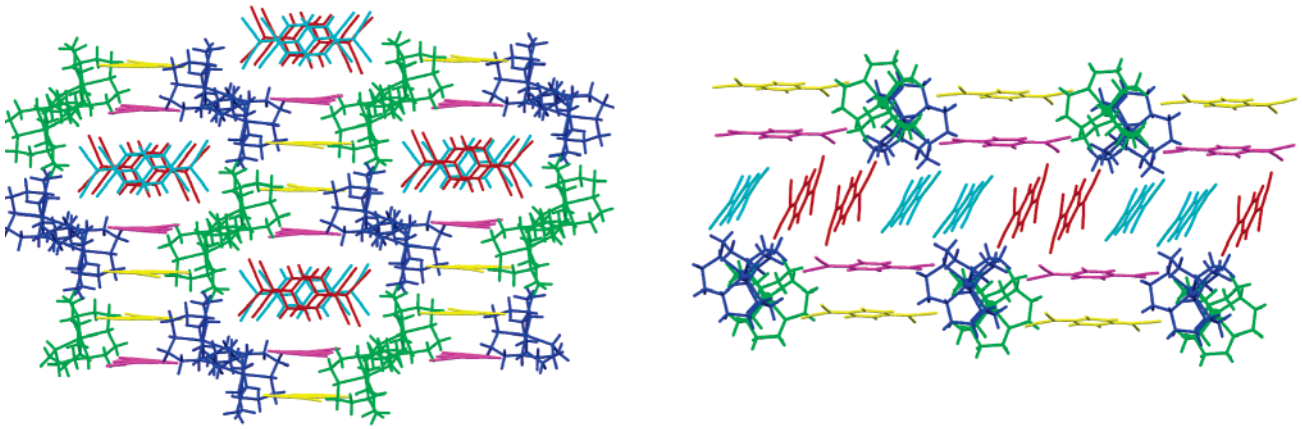

Figure 6. Two perpendicular views of the packing of **4**. TCNQ color pattern: red, A; cyan, B; yellow, C; magenta, D.

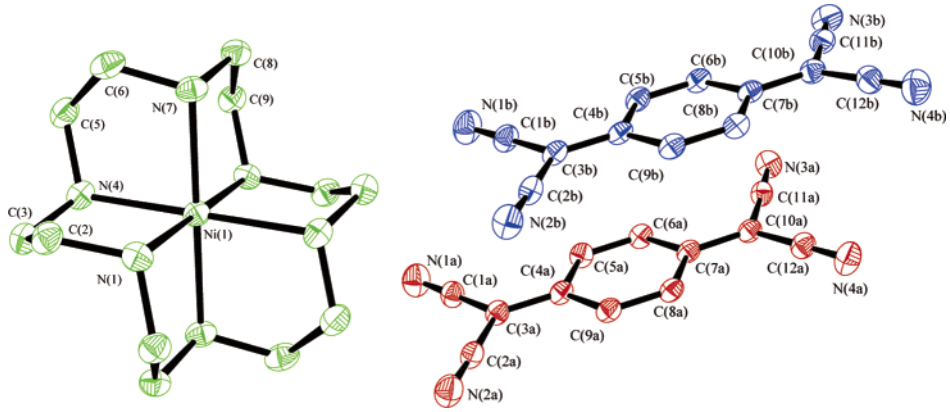

Figure 7. ORTEP view, 50% probability ellipsoids, of [Ni([18]ane-N_6)]$(TCNQ)_4$ (**6**). Color pattern: macrocyclic cation, green; TCNQ A, red; TCNQ B, blue.

Table 3. Comparative Analysis of the TCNQ Bond Distances in **6**

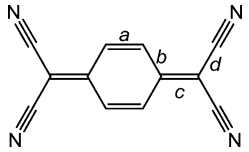

compd	*a*	*b*	*c*	*d*	*b* − *c*	*c* − *d*	*c*/(*b* + *d*)
$TCNQ^{0}$ [a]	1.345	1.448	1.374	1.441	0.074	−0.067	0.476
$TCNQ^{-}$ [a]	1.373	1.423	1.420	1.416	0.003	0.004	0.500
$TCNQ^{0.5-}$ [a]	1.354	1.434	1.396	1.428	0.040	−0.032	0.488
TCNQ A	1.359	1.437	1.396	1.434	0.041	−0.038	0.486
TCNQ B	1.363	1.434	1.403	1.429	0.031	−0.026	0.490

[a] Data taken from ref 20.

the nickel ion, k is Boltzmann's constant, β is the Bohr magneton, $x = |D|/kT$, the parameter D measuring the zero-field splitting, and $N\alpha$ is the temperature-independent paramagnetism:

$$\langle\chi\rangle = \frac{2Ng_{Ni}{}^2\beta^2}{3kT}\frac{2/x - 2\exp(-x)/x + \exp(-x)}{1 + 2\exp(-x)} + N\alpha \qquad (1)$$

The best fit (Figure 9) was obtained when $g_{Ni} = 2.179(2)$, $|D| = 3.52(8)$ cm^{-1}, and $N\alpha = 5.7(1) \times 10^{-4}$ cm^3 mol^{-1} for **1** and $g_{Ni} = 2.179(1)$, $|D| = 3.81(3)$ cm^{-1}, and $N\alpha = 3.3(1) \times 10^{-4}$ cm^3 mol^{-1}, respectively, for **4**. In both cases the values are typical of slightly distorted octahedral nickel(II) environments. The organic radicals in **4** do not contribute to the magnetic moment, indicating that dimeric $(TCNQ)_2{}^{2-}$ are formed. The dimeric dianion usually shows a strong antiferromagnetic coupling of both spins which renders the dianion diamagnetic. The magnetic susceptibility variation can then be exclusively attributed to the contribution of the isolated metal ion. The TIP values are, however, higher than expected for isolated nickel(II) ions ($(100-120) \times 10^{-6}$ cm^3 mol^{-1}) and probably are due to an overestimation of the diamagnetic correction of the sample and the sample holder.

The copper derivative **2** also follows the Curie law above 50 K with a decrease of the magnetic moment value below this temperature (Figure 9). This deviation can be attributed

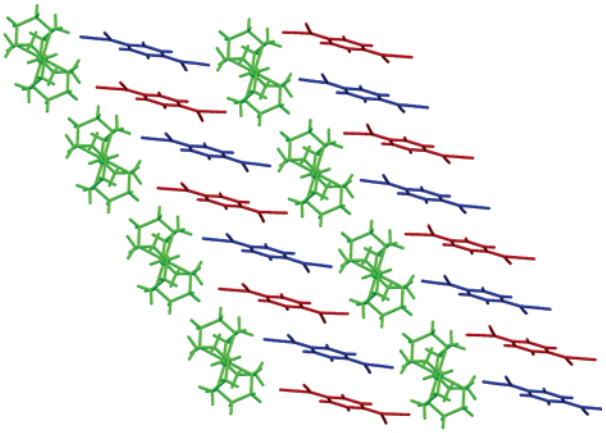

Figure 8. Packing view of **6**. TCNQ color pattern: A, red; B, blue.

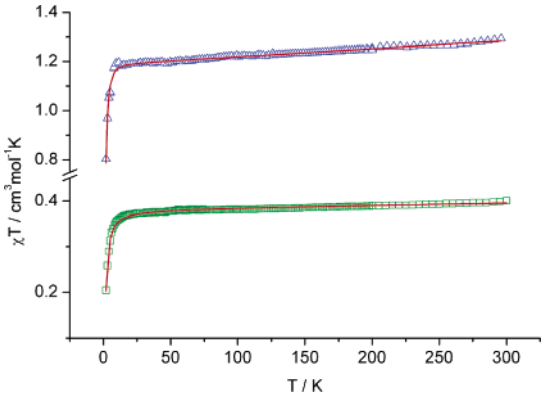

Figure 9. Temperature dependence of χT for **2**, green squares, and **4**, blue triangles. The solid lines represent the best fit using the equations described in the text.

to an antiferromagnetic coupling between the two copper atoms in the complex core. The angle Cu−Cl−Cu of 76.68° agrees with this observed antiferromagnetic coupling. The magnetic data can then be fitted to the expression based on sum of the general isotropic exchange Hamiltonian for two interacting $S = 1/2$ spins, $H = -2JS_1S_2$,[22] where J is the exchanging coupling constant for the copper ions and $N\alpha$ is the temperature-independent paramagnetism; the other parameters are the same as in eq 1:

$$\chi = \frac{Ng_{Cu}{}^2\beta^2}{kT}\frac{2}{3 + \exp(-2J/kT)} + N\alpha \qquad (2)$$

The best fit for the experimental data corresponds to $g_{Cu} = 2.016(1)$, $J = -1.052(9)$ cm^{-1}, and $N\alpha = 5.0(2) \times 10^{-5}$ cm^3 mol^{-1}, confirming a weak coupling between the copper ions.

In contrast, compounds **3** and **5** follow the Curie−Weiss law in the whole range of temperatures, indicating that the magnetic susceptibility only arises from the contribution of isolated copper(II) ions. The magnetic moment for compound **3** is 1.85 β (equivalent to $g_{Cu} = 2.14$), with a Weiss constant $\Theta = -1.18$ K. For compound **5** the correspondent values are 1.77 β ($g_{Cu} = 2.04$) and $\Theta = -0.22$ K. These values

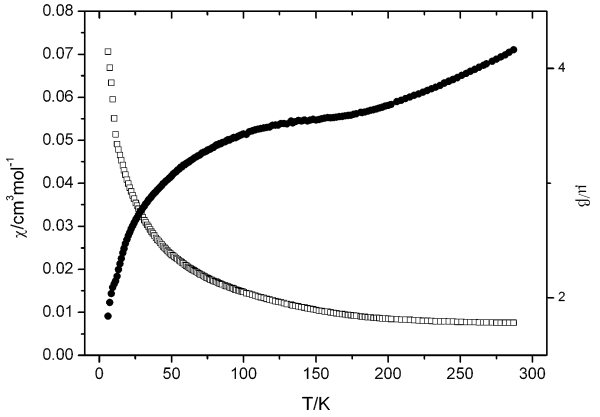

Figure 10. Temperature dependence of the susceptibility and the magnetic moment for 7.

indicate that the TCNQ radicals do not contribute to the total susceptibility, suggesting its complete dimerization in the solid.

The copper derivative with four TCNQ units, **7**, shows, on the contrary, a small contribution from the organic radicals to the total magnetic susceptibility. The magnetic moment of this compound (Figure 10) decreases from 4.16 β at 300 K to 1.72 β at 5 K. These values suggest that at lower temperatures only the metal ion contributes to the magnetic susceptibility with the spins on the TCNQ antiferromagnetically coupled and that at high temperatures three $S = 1/2$ spins are present in the formula unit, one corresponding to the copper ion and the other two to the TCNQ groups. Assuming the formation of TCNQ chains in the solid, in a way similar to that found for the nickel compound **6**, the total susceptibility can be interpreted as the sum of three terms:

$$\chi_{total} = \chi_{Cu} + \chi_{TCNQ} + N\alpha \qquad (3)$$

Here the first term corresponds to the Curie contribution of the copper(II) ions, the second one is the contribution of the organic part, and the last one is the temperature-independent paramagnetism.

Since the low-temperature values correspond exclusively to the contribution of the metal-located spins, we have fit the susceptibility values below 50 K to the sum of the Curie law and a TIP to estimate the copper contribution. From this fit a Curie constant of 0.384 cm^3 K mol^{-1} has been obtained, corresponding to a g_{Cu} value of 2.023; we also estimated the TIP as $N\alpha = 9.4 \times 10^{-4}$ cm^3 mol^{-1}. This value is in the range observed for the Pauli paramagnetism found in TCNQ derivatives with delocalized electrons[9] and other conducting radical salts.[23]

When these two contributions are subtracted from the total susceptibility, we obtain the contribution of the organic part, reported in Figure 11. It shows a maximum centered at $T \approx 19$ K, a typical feature of one-dimensional $S = 1/2$ spin systems. The experimental data have been then fitted to an

(22) Bleaney, B.; Bowers, K. D. *Proc. R. Soc. London, Ser. A* **1952**, *214*, 451.

(23) Williams, J. M.; Ferraro, J. R.; Thorn, R. J.; Carlson, K. D.; Geiser, U.; Wang, H. H.; Kini, A. M.; Whangbo, M. H. *Organic Superconductors. Synthesis, Structure, Properties, and Theory*; Grimes, R. N., Ed.; Prentice Hall: Englewood Cliffs, NJ, 1992.

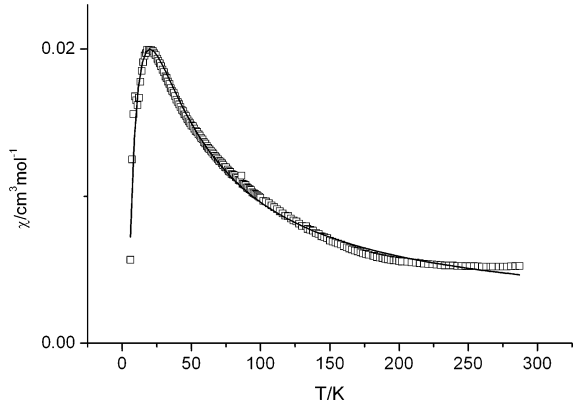

Figure 11. Plot of the TCNQ contribution to the magnetic susceptibility for **7**. The solid line is the fit to the experimental data as described in the text.

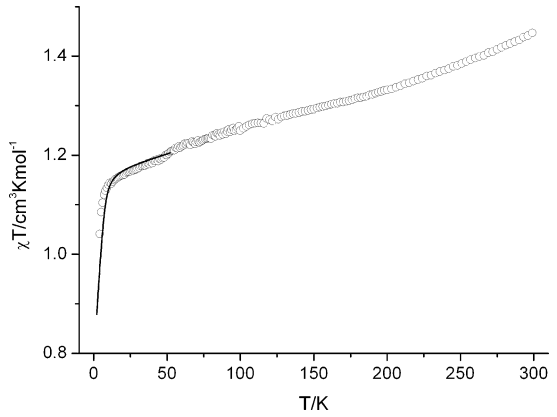

Figure 12. Temperature dependence of χT for **6**. The solid line is the fit to the experimental data below 50 K as described in the text.

alternating Heisenberg lineal chain model, $H = -J\Sigma(S_{2i-1}S_{2i} + \alpha S_{2i}S_{2i+1})$,[24] where J is the exchanging coupling constant for the TCNQ ions and α is a parameter that takes into account the distortion in the chain and can vary from $\alpha = 0$, corresponding to isolated $(TCNQ)_2^{2-}$, to $\alpha = 1$, corresponding to a uniform chain of $S = 1/2$ spins. The best fit was obtained for $J = -24.2(2)$ cm^{-1} and $\alpha = 0.77(1)$ and keeping g_{TCNQ} fixed to 2.002. These data suggest the presence of a slightly distorted magnetic chain and can indicate that TCNQ stacks similar to that described for **6** would be present in the crystal. However, the X-ray powder diffraction diagrams of **6** and **7** show no apparent relation between them, precluding further conclusions on the structure of the copper derivative.

The variation of χT with the temperature for **6** is shown in Figure 12. As in the previous compound, the magnetic behavior can be interpreted as the sum of three contributions: (i) the contribution of the nickel ion which follows the Curie law above 15 K and shows the deviation due to a zero field splitting of the ground state below this temperature; (ii) the contribution of the $S = 1/2$ spins located on the TCNQ; (iii) a temperature-independent paramagnetism.

To estimate the contributions of the nickel(II) ions and the TIP to the total susceptibility, we have fitted the data below 50 K to eq 1, and the best fit corresponds to $g_{Ni} = 2.154(1)$, $|D| = 5.11(9)$ cm^{-1}, and $N\alpha = 9.0(1) \times 10^{-4}$ cm^3 mol^{-1}. The higher D parameter compared to those obtained for **1** and **4** can be attributed to the different coordinative environment of the nickel atom, a facial isomer in **6** and a meridional isomer in **4**. The TIP value is similar to that found for **6** and in the expected range for a partially delocalized TCNQ stack. The crystal structure of this derivative suggests that the TCNQ contribution should fit to a model of interacting spins along a 1D chain. However, the magnetic data do not fit well with this model and this fact, also observed previously by us,[10b] can probably be attributed to the higher contribution of the nickel(II) ion to the total magnetic susceptibility which makes it very difficult to isolate the TCNQ contribution of the susceptibility and can lead to erroneous interpretations of the global data.

Conclusion

Several metallomacrocycles of nickel(II) and copper(II) are isolated and characterized. The large size hexaaza-macrocyclic ligand [18]ane-N_6 stabilizes copper derivatives with one or two metal ions in the macrocyclic cavity. The obtained structures show a complex network of hydrogen bonds involving chloride anions and crystallization water molecules which stabilize the supramolecular architecture.

Only mononuclear derivatives are obtained in the reaction of these species with TCNQ. Compounds of formula [M([18]-ane-N_6)](TCNQ)$_2$ appear when LiTCNQ, a source of radical-anionic TCNQ, is used. The crystal structure of the nickel derivative, **4**, indicates that the main interactions are the electrostatic attractions between cationic metallomacrocycles and dimeric dianions $(TCNQ)_2^{2-}$, which stack in the solid. A different type of compound, with general formula [M([18]-ane-N_6)](TCNQ)$_4$, is obtained in the reaction with (Et_3NH)-$(TCNQ)_2$. The reagent has one unpaired electron delocalized between two TCNQ units, and this proportion is maintained in the final derivatives. The nickel derivative, **6**, shows the TCNQ stacked along the crystal with partial electronic delocalization, as the alternate TCNQ−TCNQ interplanar distances indicate. A noticeable fact is the formation of different metallomacrocyclic isomers depending on the number of TCNQ units present in the formula. The *mer* isomer corresponds to the derivative with two TCNQ/ formula, while the *fac* isomer appears in the partially reduced TCNQ derivative. The reason for this change could be in the different size of the metallomacrocyclic unit in relation with the space available to accommodate the TCNQ groups since the facial isomer has a flattened and elongated shape in contrast to the more spherical *mer* isomer, which seems to be the more stable form.

The magnetic susceptibility data of the TCNQ derivatives show that the TCNQ anions forming dimeric $(TCNQ)_2^{2-}$ are antiferromagnetically coupled rendering diamagnetic units

(24) Hall, J. W.; Marsh, W. E.; Weller, R. R.; Hatfield, W. E. *Inorg. Chem.* **1981**, *20*, 1033−1037.

in the whole range of temperatures. In the derivatives having four TCNQ/formula unit, especially in the copper derivative, the partially reduced TCNQ are stacked giving rise to some degree of electronic delocalization. This fact results in smaller antiferromagnetic interactions interpreted in terms of an alternated chain of interacting $S = 1/2$ spins. The same behavior has been previously observed by us in other derivatives having stacked $TCNQ^{0.5-}$.[10]

Acknowledgment. We gratefully acknowledge the Spanish Comunidad Autónoma de Madrid, Projects S0505/PPQ/0316 and UCM2005-910300, for financial support.

Supporting Information Available: Crystallographic data for compounds **2**−**4** and **6** in CIF format and fits of the magnetic data for the obtained compounds. This material is available free of charge via the Internet at http://pubs.acs.org.

IC062016H